Thermal point-contact spectroscopy in UPt_3

A. A. Lysykh,* A. M. Duif, A. G. M. Jansen, and P. Wyder
Max-Planck-Institut für Festkörperforschung, Hochfeld-Magnetlabor, 25 Avenue des Martyrs, Boîte Postale 166X, F-38042 Grenoble Cédex, France

A. de Visser
Centre des Recherches sur les Très Basses Températures, Centre National de la Recherche Scientifique, Boîte Postale 166X, F-38042 Grenoble Cédex, France

(Received 7 December 1987)

The current-voltage characteristics of UPt_3 point contacts have been measured between 4 and 100 K. The voltage dependence of the contact resistance at low temperatures resembles the temperature dependence of the resistance at zero bias voltage. These point-contact data are explained in terms of local Joule heating in the contact area.

Point-contact spectroscopy is used to study the energy dependence of the interaction of electrons with elementary excitations in a metal.[1,2] Mainly this technique has been applied for a direct determination of the Eliashberg function for the electron-phonon coupling from the measured nonlinearity in the current-voltage characteristic of a metallic point contact. For a long list of materials[1] point-contact spectroscopy has been applied successfully to the study of the electron-phonon interaction. Recently, point contacts have been used for the study of less common compounds with rare earths and actinides.[3–6] Valence fluctuations and heavy fermions are very interesting phenomena in these systems. Structure in the current-voltage characteristics of point contacts with these systems have been analyzed in terms of electron-scattering with valence fluctuations[3] and density-of-states effects.[4–6] However, alternative explanations have been raised in a description of local heating of the contact area.[7,8] In an introduction we will sketch the problem by mentioning the relevant dimensional parameters, i.e., contact dimension with respect to the mean free path of the electrons, and their influence in a point-contact experiment. We will discuss the effect of an energy-dependent density of states on the nonlinearity of a current-voltage characteristic for a point contact. Experimentally, we investigated point contacts of the heavy-fermion system UPt_3 as a function of temperature between 4 and 100 K. Others reported point-contact experiments on UPt_3 with the interpretation in a simple model for the spectroscopy of the density of states.[9] We will apply the model with local heating of the contact area to analyze the results.

I. DIMENSIONAL CRITERIA

Important parameters in the evaluation of point-contact experiments are the contact dimension and the mean free path of the electrons. The contact dimension can be defined by the radius a of a circular contact between two semi-infinite metallic parts. For the mean free path of the electrons we consider the inelastic scattering of the electrons, given by the inelastic scattering length l_ε or the inelastic diffusion length $\Lambda_\varepsilon=(l_\varepsilon l_i)^{1/2}$ for the case of strong elastic scattering (mean free path l_i). The inelastic mean free path depends on the electron energy ε with respect to the Fermi level.

In the regime where $l_\varepsilon, l_i \gg a$, electrons are injected ballistically through the contact in the presence of an applied voltage V. The relevant electron mean free path l_ε is then determined by the energy $\varepsilon=eV$. In this so-called ballistic regime we can obtain in an optimum way spectroscopic information of the scattering of electrons. The nonequilibrium distribution of the ballistically injected electrons relaxes via the spontaneous emission of phonons, yielding voltage-dependent corrections to the current. The spectroscopic information is measured directly in the second derivative d^2I/dV^2 of the current I with respect to the voltage V via the expression[1,2]

$$\frac{d^2I}{dV^2} \propto a^3\alpha^2F(eV) \ . \tag{1}$$

The voltage-dependent d^2I/dV^2 signal is proportional to the Eliashberg function α^2F for the electron-phonon interaction. The above-described inelastic scattering of the electrons contributes to the signal most efficiently for processes occurring in the contact region, yielding the contact volume a^3 in the proportionality of Eq. (1).

In the diffusive regime where $\Lambda_\varepsilon > a > l_i$, the nonequilibrium distribution of the electrons is similar in energy space as for the ballistic regime. Only the momenta are randomized due to elastic scattering. The spectroscopic information is again given by Eq. (1). The factor a^3 in Eq. (1) has to be multiplied by a factor l_i/a which results in a smaller efficiency volume equal to a^2l_i.[10] Thus with small elastic mean free paths as in metallic alloys, it is still possible to do phonon spectroscopy; however, with a decreased intensity of the measured signals.[11] Note that in the ballistic and diffusive regime the Joule heat is released in a volume (defined by l_ε or Λ_ε) greater than the contact area. In the first order heating effects can be

 ©1988 The American Physical Society

neglected in the interpretation of the non-Ohmic behavior in these clean contacts.

In the thermal regime where $a \gg l_\varepsilon, l_i$, it is no longer possible to do energy resolved spectroscopy in a point-contact experiment. Due to the strong scattering, the electron and phonon systems are in equilibrium. Joule heating of the contact area cannot be ignored. Already in 1900 Kohlrausch solved this problem for an arbitrary contact geometry.[12] Assuming equal flow lines for electrical and thermal conduction, the following relation exists between the applied voltage V and the maximum temperature $T_{\max}$ at the center of a contact at a temperature T_{bath}:

$$V^2 = 8 \int_{T_{\text{bath}}}^{T_{\max}} \rho\lambda \, dT \ , \tag{2}$$

where ρ and λ are, respectively, the electrical resistivity and thermal conductivity of the bulk material. Because the equipotential surfaces coincide with the surfaces of constant temperature, this relation contains no factor depending on the specific geometry of the contact. If the Wiedemann-Franz law $\rho\lambda = LT$ holds and $T_{\max} \gg T_{\text{bath}}$, then Eq. (2) gives that the maximum temperature in the contact is proportional to the applied voltage. For the Sommerfeld value of the Lorenz number L ($=2.45\times10^{-8}$ V^2/K^2) this yields a hot spot in the contact with an increase in the temperature of 3.2 K for each mV across the contact. In the thermal regime the resistance R_M of a contact is obtained from a solution of the Maxwell equations with appropriate boundary conditions yielding

$$R_M = \rho/2a \ , \tag{3}$$

for a circular contact of radius a. For a dirty contact the voltage-dependent contact resistance resembles the temperature-dependent bulk resistivity using Eq. (2) to map the applied voltage to the contact temperature. Equation (2) gives only the maximum temperature in the contact region. For a temperature-dependent resistivity an integral of the resistivity over the temperature profile near the contact has to be taken to calculate the voltage-dependent contact resistance. As such the geometry enters the problem.[13] Because the dominant contribution of the contact resistance is given by the resistivity in the middle of a contact, a good approximation will be given by taking the resistivity at the maximum temperature instead of the detailed temperature profile. To account for the local resistivity in the contact area it is better to compare the voltage dependence of the dynamical contact resistance $dV/dI(V)$ at low temperatures with the temperature dependence of the contact resistance $R(T)$ at zero bias voltage instead of with the temperature-dependent bulk resisitivity.[7]

II. INFLUENCE OF THE DENSITY OF STATES

The heavy-fermion character at low temperatures is ascribed to the occurrence of a many-particle resonance in the density of states near the Fermi level. In an explanation of point-contact data of mixed-valence and heavy-fermion systems it has been argued that one observes the energy dependence of the electron density of states $N(\varepsilon)$ in these systems.[5,6] Analogously to the tunneling formula one often writes the current through a contact as the following integral:[5]

$$I \propto \int_0^{eV} N(\varepsilon) d\varepsilon \ . \tag{4}$$

Then, the differential conductance dI/dV is proportional to $N(eV)$. In an exact description of the point-contact problem in the ballistic limit, the density of states does not enter the problem as given in the last equation. To clarify this, we derive the resistance of a contact in the clean limit considering specific band-structure effects. In zeroth order without collisions the current I_0 through a contact can be written as[1,2]

$$I_0 = 2e \int d^2\mathbf{r} \int d^3\mathbf{k} \, v_{\mathbf{k}n} f_{\mathbf{k}}^0(\mathbf{r}) \ , \tag{5}$$

where $v_{\mathbf{k}n}$ is the velocity component normal to the contact area. The surface integral $\int d^2\mathbf{r}$ runs over the contact area and equals πa^2 for a circular contact. The electronic distribution function $f_{\mathbf{k}}^0(\mathbf{r})$ describes a filled Fermi sphere with differences in the electrochemical potential depending on the velocity direction of the electrons. At the orifice the distorted Fermi sphere consists of two filled half-spheres with energy radii $(E_F + eV/2$ and $E_F - eV/2$. Evaluating Eq. (5) in the limit of low temperatures we get

$$I_0 = \frac{e}{4\hbar\pi^3} \pi a^2 \int_{E_F - eV/2}^{E_F + eV/2} d\varepsilon \int_{\varepsilon = \varepsilon_{\mathbf{k}}} dS_{\mathbf{k}} \, | \, \mathbf{n}_{\mathbf{k}} \cdot \mathbf{s} \, | \ . \tag{6}$$

$dS_{\mathbf{k}}$ is an infinitesimal area on the Fermi surface with constant energy ε (the integration is only over half the Fermi sphere). $\mathbf{n}_{\mathbf{k}}$ and $\mathbf{s}$ are unit vectors, respectively, parallel to $\mathbf{v}_{\mathbf{k}}$ and perpendicular to the contact surface. The current is proportional to a projection of the Fermi surface on the plane of the contact. For an average over all orientations of the crystal with respect to the contact we take $| \, \mathbf{n}_{\mathbf{k}} \cdot \mathbf{s} \, | = \frac{1}{2}$, which is exact for the isotropic case. As a result for the differential conductance dI_0/dV we get

$$\frac{dI_0}{dV} = \frac{e^2}{32\hbar\pi^3} \pi a^2 [S(E_F + eV/2) + S(E_F - eV/2)] \ , \tag{7}$$

where $S(E)$ is the energy-dependent area of the Fermi surface. In Eq. (7) we have added a factor $\frac{1}{2}$ for the area $S(E)$ to be related to the total Fermi sphere. For a quadratic dispersion relation $[S(E) \propto E]$, the contact resistance is independent of the applied voltage and equals the Sharvin[14] formula $R_{\text{Sh}} = 4\rho l/3\pi a^2$ for the resistance of a clean contact; here, we have used $\rho l = m v_F / n_0 e^2$ with the electron concentration $n_0 = k_F^3/3\pi^2$. For a nonquadratic dispersion relation the voltage derivative of the conductance of the contact may depend on the applied voltage via the asymmetry in the effective mass $[m(E) \propto dS/dE]$ around the Fermi level. In the point-contact problem the density of states does not show up in the simple description given by Eq. (4). In terms of the Fermi-surface area $S(E)$ the density of states can be written as $N(E) \propto S^{1/2} dS/dE$. Nonquadratic dispersion and anisotropy are important to include band-structure and mass-

renormalization effects in the description of a point contact.

III. EXPERIMENTAL DETAILS

Point-contact experiments were performed on polycrystalline UPt_3 between 4 and 100 K using a flow cryostat. To make the contact two pieces of bulk material were pressed against each other. The current-voltage characteristics and its derivatives of the voltage with respect to the current were measured using a phase-sensitive detection technique at 500 Hz. Due to differences in thermal expansion of the various parts in the sample holder, the metallic contacts were not stable and changed continuously at a temperature above roughly 80 K. In the first attempt to do temperature-dependent experiments these disturbing effects occurred at still lower temperatures. Therefore, we mounted a spring bent from copper wire in the contact setup to reduce the induced changes in the force on the contact area upon varying the temperature.

The obtained contact resistances ranged from 0.1 to 10 Ω. Using the value for the bulk resistivity $\rho(4\ \mathrm{K})=3\times10^{-7}\ \Omega\,\mathrm{m}$ in the a-b plane of a single crystal,[15] we obtain with Eq. (3) contact radii from 1500 to 15 nm. For six f electrons in the unit cell (volume $140.9\times10^{-30}\ \mathrm{m}^3$) of UPt_3 we get the free-electron value $\rho l=\hbar k_F/n_0e^2=1.04\times10^{-15}\ \Omega\,\mathrm{m}^2$. Using this value for the product ρl we obtain a mean free path of 3 nm at 4 K. Hence, the studied contacts will be in the thermal limit ($l<a$). For the temperature-dependent measurements the resistances below 1Ω turned out to be the most stable.

IV. EXPERIMENTAL RESULTS AND DISCUSSION

In Fig. 1 we have plotted the differential resistance $dV/dI(V,T_{\mathrm{bath}})$ for a UPt_3 point contact as a function of the applied voltage V for different temperatures T_{bath} up to 100 K. The characteristics were symmetric around $V=0$. With increasing temperature the drop in resistance at bias voltages below 20 mV gradually disappears and is not visible above 25 K. For the lowest measuring temperature the differential resistance as a function of the voltage resembles the bulk resistivity as a function of the temperature.[15] The bulk resistivity of UPt_3 shows a sharp rise at low temperatures (<20 K) followed by a less strong increase at higher temperatures with a tendency to saturation in the room-temperature region. Spin-fluctuation scattering [$\rho(T)\propto T^2$] and a Kondo-lattice behavior with screening of the scattering centers play a role in the drop of the resistivity at low temperatures. Regarding the temperature dependence between 4 and 100 K, the relative change $\Delta\rho(T)/\rho$ in bulk resistivity is roughly a factor 5 larger than the relative change $\Delta R(T)/R$ in point-contact resistance at zero voltage for the data of Fig. 1. As a consequence, a determination of the contact dimension from the temperature dependence of the contact resistance yields a discrepancy with the same factor 5 as compared to the obtained contact radius from the low-temperature resistance value. This

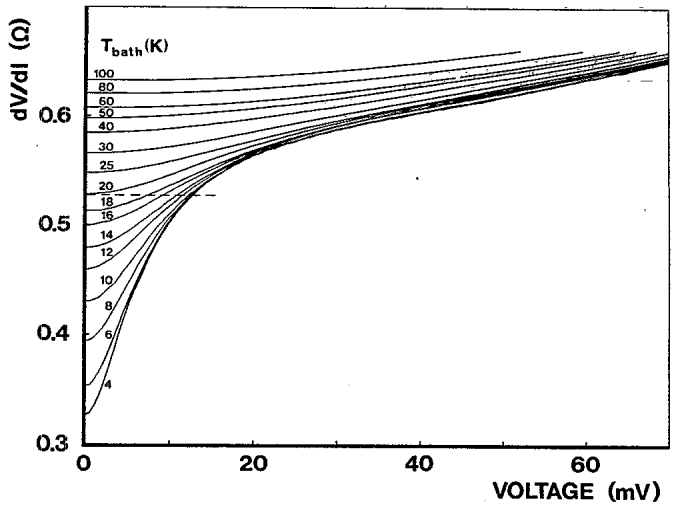

FIG. 1. Measured differential resistance dV/dI as a function of applied voltage of a UPt_3 point contact at different bath temperatures T_{bath} as indicated in the figure, showing the drop in resistance at low bias voltages which disappears at high temperatures ($T_{\mathrm{bath}}>25$ K). The dashed horizontal line serves as an example how to obtain data points in the V-T_{bath} diagram at, e.g., $T_{\max}=20$ K, plotted in Fig. 3.

discrepancy is often encountered in an analysis of the point-contact data in the thermal limit.[4,7,8] For pure metals (i.e., Cu) the two determinations show a good agreement.[16] A reason for this could be that on the local scale of the point contact the temperature-dependent resistivity deviates from the bulk value. Because of the relatively small effects of the pressure on the bulk resistivity for UPt_3,[15] it is unlikely that a distortion in the contact region fully explains this local deviation from the bulk resistivity. Although the temperature dependence of the contact resistance itself is not in detail understood from the temperature-dependent resistivity, we will analyze the voltage-dependent contact resistance quantitatively by the use of the temperature dependence of the contact resistance instead of that of the bulk resistivity.

In Fig. 2 the dynamical resistance $dV/dI(V,T_{\mathrm{bath}}=4\ \mathrm{K})$ has been plotted together with the data points of $dV/dI(V=0,T_{\mathrm{bath}})$. For the scaling of the temperature with respect to the voltage scale we used Eq. (2). Due to the strong electron-electron scattering in UPt_3 the thermal conductivity of the phonons has a significant contribution and this results in a Lorenz number with a value higher than the Sommerfeld value. From the measured temperature dependence of the specific resistivity and the thermal conductivity of bulk UPt_3 the temperature-dependent Lorenz number has been determined.[17] With these experimental data we calculated with Eq. (2) the relation between the maximal temperature in the contact and the applied voltage. Using this scaling between voltage and temperature (roughly 1.5 K increase in temperature for each mV), we see in Fig. 2 good agreement between the curve of $dV/dI(V,T_{\mathrm{bath}}=4\ \mathrm{K})$ and the data points of $dV/dI(V=0,T_{\mathrm{bath}})$. The data above 80 K are less reliable because of the aforemen-

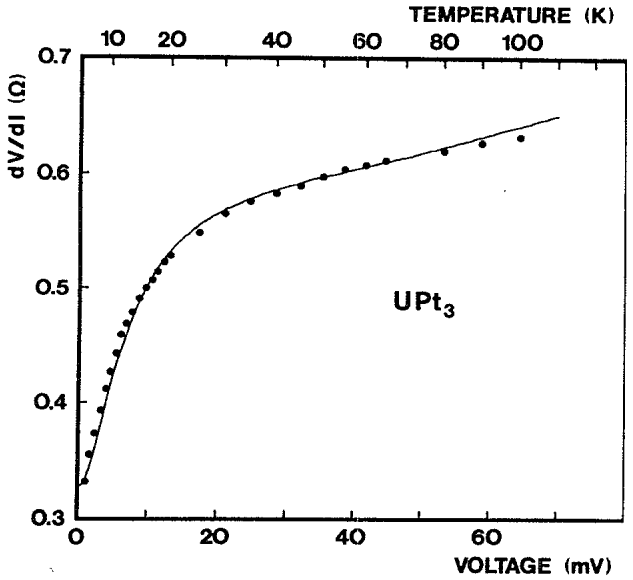

FIG. 2. Comparison between the voltage-dependent differential resistance $dV/dI(V, T_{bath}=4\ K)$ of a UPt_3 point contact (solid line) and its temperature-dependent differential resistance $dV/dI(V=0, T_{bath})$ (dots). The heating model has been used for the scaling between temperature and voltage.

tioned difficulties in preserving the same contact.

A comparison of $dV/dI(V, T_{bath}=\text{const})$ and $dV/dI(V=0, T_{bath})$ can be done for the measurements at all bath temperatures by the corresponding scaling between voltage and temperature in Eq. (2). Graphically this comparison has been realized for all temperatures in Fig. 3. Using Eq. (2) with the temperature-dependent transport data, we have drawn in the V-T_{bath} diagram curves with a constant temperature T_{max} in the center of the contact. From the data in Fig. 1 a set of data points V-T_{bath} can be obtained for a certain T_{max} by taking $dV/dI(V=0, T_{max})$ equal to $dV/dI(V, T_{bath})$. An example of this is given by the dashed line in Fig. 1, which corresponds with a maximum temperature $T_{max}=20$ K. The points where this dashed line intersects the experimental curves give the V-T_{bath} points near the $T_{max}=20$ K line in Fig. 3. Again we see that the data show a good agreement for temperatures up to 60 K.

To look at the reproducibility we plotted in Fig. 4 the voltage derivative $d(dV/dI)/dV$ of the dynamical resistance as a function of the voltage for different point contacts at low temperatures ($\simeq 4$ K). For comparison we also have drawn the temperature derivative of the bulk resistivity in the a-b plane of UPt_3 as a function of the temperature.[15] The amplitudes of $d(dV/dI)/dV$ were adjusted to coincide with the temperature-dependent data in the region between 10 and 20 mV. Again we used mapping between voltage and temperature as discussed before. As can be seen in Fig. 4, there is a difference in the observed nonlinearity from contact to contact. We believe that the local pressure and deformation in the contact area plays a role for the understanding of this effect. A realistic force of 10^{-3} kgf on an area of 10 μm^2 gives already a pressure of 10 kbar on the contact. In the same way, the $d\rho/dT$ curve of the resistivity shows a shift of the maximum (0.35 K/kbar) with increasing pressure.[15]

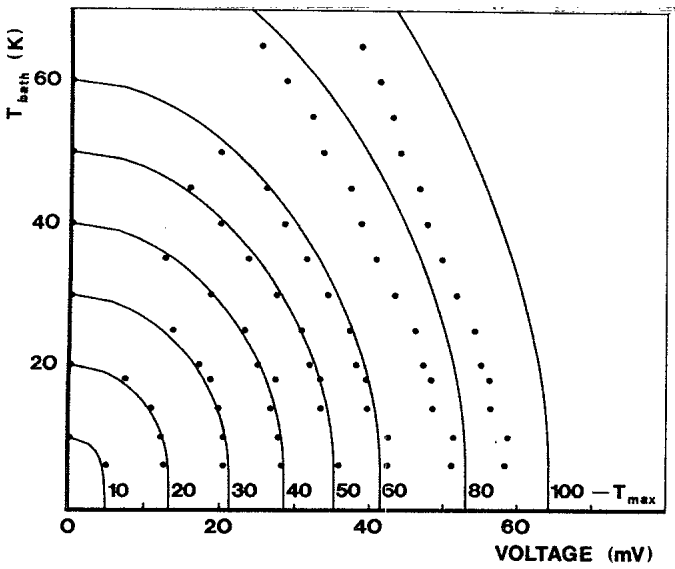

FIG. 3. Calculated curves in the V-T_{bath} plane with the indicated temperature T_{max} at the center of a UPt_3 point contact according to the heating model, using Eq. (2). The dots represent the values of the voltage and bath temperature belonging to a point on the curves of Fig. 1, where the resistance is equal to the resistance at zero voltage (in Fig. 1, the points of intersection of the dashed line with the experimental curves give the set of data for $T_{max}=20$ K).

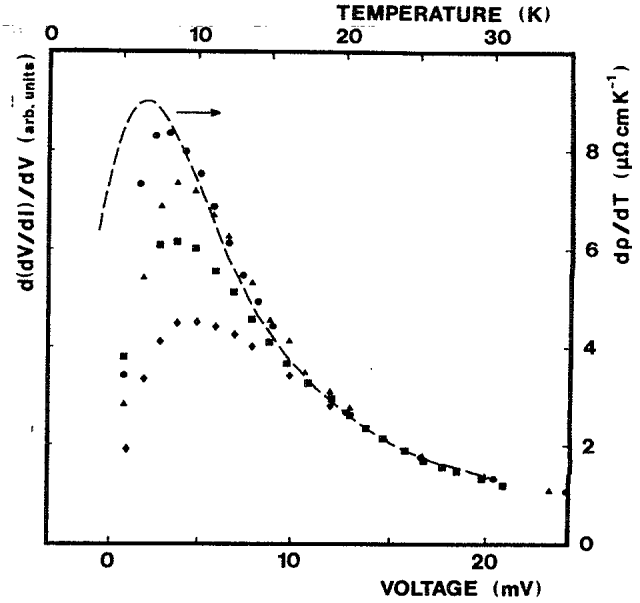

FIG. 4. Comparison of the voltage derivative of the differential resistance $d(dV/dI)/dV$ as a function of applied voltage for different UPt_3 point contacts at $T=4.2$ K (dots) with the temperature derivative of the bulk resistivity $d\rho/dT$ in the a-b plane of UPt_3 as a function of temperature (dashed line, after Ref. 15). The heating model has been used for the scaling between temperature and voltage.

V. CONCLUSIONS

Due to the strong scattering of electrons in UPt_3 the point contacts with this heavy-fermion system are in the dirty limit ($l < a$). For UPt_3, the measured nonlinear point-contact characteristics can be described in a model of Joule heating in the contact area by a comparison with the temperature-dependent contact resistance. As should be for the thermal limit, the relative change of contact resistance with temperature cannot be explained quantitatively from the temperature-dependent resistivity. However, the functional temperature dependencies are similar for the contact resistance and the bulk resistivity. Local heating of the point contact can be neglected in pure contacts ($l > a$). For contacts in this limit, the voltage dependence of the resistance is quite different from the temperature dependence.[18]

Also for other metals with narrow-band phenomena (heavy fermions, mixed valences) heating of the contact has to be considered in the interpretation of the point-contact data. It will depend on the specific system under study to what extent the heating model has to be taken into account for point-contact experiments.

The energy dependence of the density of states cancels against the electron velocity in a simple free-electron description of the voltage dependence of the resistance of a clean contact. In order to see any influence of the electronic band structure in the point-contact spectra, a detailed theory should include nonparabolicity and anisotropy of the electronic bands.

ACKNOWLEDGMENTS

Part of this work has been supported by the Stichting voor Fundamenteel Onderzoek der Materie (Foundation for Fundamental Research on Matter) with financial support from the Nederlandse Organisatie voor Zuiver Wetenschappelijk Onderzoek (Netherlands Organization for the Advancement of Pure Research).

*Permanent address: Institute for Low Temperature Physics and Engineering, Ukrainian S.S.R. Academy of Sciences, 47 Lenin Avenue, Kharkov, USSR.

[1]I. K. Yanson, Fiz. Nizk. Temp. **9**, 676 (1983) [Sov. J. Low Temp. Phys. **9**, 343 (1983)].

[2]A. G. M. Jansen, A. P. van Gelder, and P. Wyder, J. Phys. C **13**, 6073 (1980).

[3]B. Bussian, I. Frankowski, and D. Wohlleben, Phys. Rev. Lett. **49**, 1026 (1982).

[4]E. Paulus and G. Voss, J. Magn. Magn. Mater. **47&48**, 539 (1985).

[5]I. Frankowski and P. Wachter, Solid State Commun. **41**, 577 (1985).

[6]M. Moser, P. Wachter, F. Hulliger, and J. R. Etourneau, Solid State Commun. **54**, 241 (1985).

[7]Yu. G. Neidyuk, N. N. Grivbov, A. A. Lysykh, I. K. Yanson, N. B. Brandt, and V. V. Moshchalkov, Pis'ma Zh. Eksp. Teor. Fiz. **41**, 325 (1985) [JETP Lett. **41**, 399 (1985)].

[8]A. G. M. Jansen, A. de Visser, A. M. Duif, J. J. M. Franse, and J. A. A. J. Perenboom, J. Magn. Magn. Mater. **63&64**, 670 (1987).

[9]M. Moser, P. Wachter, and J. J. M. Franse, Solid State Commun. **58**, 515 (1986).

[10]I. O. Kulik and I. K. Yanson, Fiz. Nizk. Temp. **4**, 1267 (1978) [Sov. J. Low Temp. Phys. **4**, 596 (1978)].

[11]A. Lysykh, I. K. Yanson, O. I. Shklyarevski, and Yu. G. Naydyuk, Solid State Commun. **35**, 987 (1980).

[12]R. Holm, *Electric Contacts* (Springer-Verlag, Berlin, 1967).

[13]J. A. Greenwood and J. B. P. Williamson, Proc. R. Soc. London, Ser. A **246**, 13 (1958).

[14]Yu. V. Sharvin, Zh, Eksp. Teor. Fiz. **48**, 984 (1965) [Sov. Phys.—JETP **21**, 655 (1965)].

[15]A. de Visser, J. J. M. Franse, and A. Menovsky, J. Magn. Magn. Mater. **43**, 43 (1984).

[16]A. P. van Gelder, A. G. M. Jansen, and P. Wyder, Phys. Rev. B **22**, 1515 (1980).

[17]J. J. M. Franse, A. Menovsky, A. de Visser, C. D. Bredl, U. Gottwich, W. Lieke, H. M. Mayer, U. Rauchschwalbe, G. Sparn, and F. Steglich, Z. Phys. B **59**, 15 (1985).

[18]A. G. M. Jansen, A. M. Duif, A. A. Lysykh, and P. Wyder, in *Narrow Band Phenomena, Staverden, The Netherlands (1987), NATO Advanced Study Workshop,* edited by J. C. Fuggle and G. Sawatzky (Plenum, New York, in press).